Statistical Analysis and Stochastic Simulation of Ground-Motion Data

By S. C. LIU

(Manuscript received July 31, 1968)

The time variations of the root-mean-square accelerations, the autocorrelation functions, and the power spectral density functions of 12 strong-motion earthquake accelerograms are analyzed. The results indicate that: (i) strong-motion accelerograms of sufficiently long duration are stationary in the rms sense, (ii) the stationary rms acceleration is a good measurement of earthquake intensity, and (iii) the autocorrelation and power spectral density functions of strong-motion accelerograms resemble those of a narrowband process. Based upon these results, a method of determining the transfer characteristics of a site is introduced. A procedure for generating a filtered, gaussian stationary process to simulate ground motions is developed, and two applications of this simulation procedure illustrate its significance.

I. INTRODUCTION

For many years structural engineers have been concerned with the dynamic response of structural systems subjected to seismic excitations. Ground motions may be caused by natural earthquakes, by underground explosions, or by nuclear air blasts. Structures such as high-rise buildings, nuclear reactor facilities, or sensitive equipment in the vicinity of such events are vulnerable to induced random-type disturbances. Traditionally, deterministic methods of analysis relying on the known earthquake response spectra have been used.[1] These methods have provided valuable information regarding the behavior of structures during earthquakes. However, this procedure has a serious restriction in that only a few strong-motion accelerograms exist which provide ground-motion input. An earthquake is usually initiated by a series of irregular slippages along faults, followed by

innumerable random reflections, refractions, dispersions, and attenuations of the seismic waves within the complex ground formations through which they travel.

Since ground motions are generally random, a probabilistic method of analysis appears to be more appropriate than the traditional method of establishing a reliable design basis for structures subjected to ground motions. The simulation of ground motion is undoubtedly a necessary step in performing such a probabilistic analysis. Because earthquakes are unpredictable, some researchers in structural and earthquake engineering have attempted in recent years to simulate earthquakes by using stochastic processes. Both stationary and nonstationary models have been investigated.[2–8]

It is the purpose of this paper to investigate the best characterization of ground motions and to establish a valid basis for the stochastic simulation of seismic records. For this purpose, 12 commonly used strong-motion earthquake accelerograms are analyzed. The time variations of the rms accelerations, the autocorrelation functions, and the power spectral density functions of these accelerograms are investigated. The stationary rms accelerations are used as a measure of earthquake intensities and are compared with those found by Housner.[9] From the power spectral density analysis of existing ground-motion records, a linear filter can be determined to represent the transfer characteristics of the ground layers at a particular site. This filter is used in developing a method of generating a gaussian stationary process to simulate ground-motion accelerations.

In Section III the generation of synthetic ground acceleration records using a digital computer is discussed. The synthetic records are generated from existing records and from estimated response spectra. Two practical examples, of importance to structural engineering, are illustrated in Section IV.

II. STATISTICAL ANALYSIS OF GROUND-MOTION DATA

In general, no individual record is representative of any other record in an ensemble. However, if the data are stationary, valuable statistics may be derived by averaging the existing records. If an ergodic process is considered, a single record will be sufficient to represent the entire process.

The mean value of a given time-history record $x(t)$ of duration T is defined by

$$\langle x \rangle_{\text{av}} = \frac{1}{T} \int_0^T x(t)\, dt. \tag{1}$$

The mean square value of $x(t)$ is defined by

$$\langle x^2 \rangle_{av} = \frac{1}{T} \int_0^T x^2(t)\, dt. \tag{2}$$

Following this definition, the root-mean-square or the rms value of $x(t)$ is the positive square root of the mean square value $\langle x^2 \rangle_{av}$. This is given by

$$\text{rms of } x(t) = \left[\frac{1}{T} \int_0^T x^2(t)\, dt \right]^{\frac{1}{2}} \tag{3}$$

If $x(t)$ is a stationary random process with zero mean, its autocorrelation function $R_x(\tau)$ and power spectral density function $S_x(\omega)$ are given by the following transform pair:

$$R_x(\tau) = \lim_{T \to \infty} \frac{1}{T} \int_0^T x(t)x(t + \tau)\, dt. \tag{4}$$

$$S_x(\omega) = \frac{1}{2\pi} \int_{-\infty}^{\infty} R_x(\tau) e^{-i\omega\tau}\, d\tau. \tag{5}$$

Notice that $R_x(\tau)$ is always a real-value even function with a maximum at $\tau = 0$ and that, if $\langle x \rangle_{av} = 0$,

$$R_x(0) = \int_{-\infty}^{\infty} S_x(\omega)\, d\omega = \lim_{T \to \infty} \langle x^2 \rangle_{av}\ , \tag{6}$$

that is, the maximum autocorrelation represents the mean square value of a stationary random process.

These simple statistical quantities defined in equations 1 through 5 are useful in applying random vibration theory in earthquake engineering. The mean value, mean square value, and root-mean-square value represent the time-average strength of the input function. The timt variations of $\langle x \rangle_{av}$, $\langle x^2 \rangle_{av}$, or rms of $x(t)$ can be used to test the restricted sense stationarity of a time series. The autocorrelation function and the power spectral density function are closely related to the second-order properties and are generally used as characterization functions of a stationary process. Since strong-motion earthquake accelerograms are, in general, gaussian,[5] either the autocorrelation functions or the power spectral density functions will be sufficient to provide a complete statistical description. These two functions also provide a mathematical basis for the random response analysis of linear structural systems.

If $x(t)$ is given in digitized form, equations 1 through 5 can be

written respectively as follows:

$$\langle x \rangle_{av} = \frac{1}{N} \sum_{k=1}^{N} x_k \,, \tag{7}$$

$$\langle x^2 \rangle_{av} = \frac{1}{N} \sum_{k=1}^{N} x_k^2 \,, \tag{8}$$

$$\text{rms of } x(t) = \left[\frac{1}{N} \sum_{k=1}^{N} x_k^2 \right]^{\frac{1}{2}}, \tag{9}$$

$$R_k = R_x(k\,\Delta t) = \frac{1}{N-k} \sum_{j=1}^{N-k} x_j x_{j+k} \,, \qquad k = 0, 1, 2, \cdots, m, \tag{10}$$

and

$$S_k = S_x(\omega) = \frac{\Delta t}{\pi} \left[R_o + 2 \sum_{j=1}^{m-1} R_j \cos \frac{\pi j k}{m} + (-1)^k R_m \right], \qquad k = 0, 1, 2, \cdots, m, \tag{11}$$

in which $N = T/\Delta t$ equals the digitization time interval Δt, $x_k = x(k\Delta t)$, and m represents the maximum lag number.

2.1 *Six Strong-Motion Earthquakes*

Using equations 7 through 11, six commonly used strong-motion earthquakes each with two horizontal components are analyzed. They are:

A. El Centro, California, December 30, 1934, N-S.
B. The same, but E-W.
C. El Centro, California, May 18, 1940, N-S.
D. The same, but E-W.
E. Olympia, Washington, April 13, 1949, S10E.
F. The same, but S80W.
G. Taft, California, July 21, 1952, S21W.
H. The same, but N69W.
I. Golden Gate Park, San Francisco, March 22, 1957, N10E.
J. The same, but S80E.
K. Alameda Park, Mexico City, May 11, 1962, N10°46′W.
L. The same, but N79°14′E.

The accelerograms for these earthquakes are presented in Fig. 1. Upon first inspecting these existing strong-motion accelerograms, one might conclude that they are nonstationary. However, this conclusion

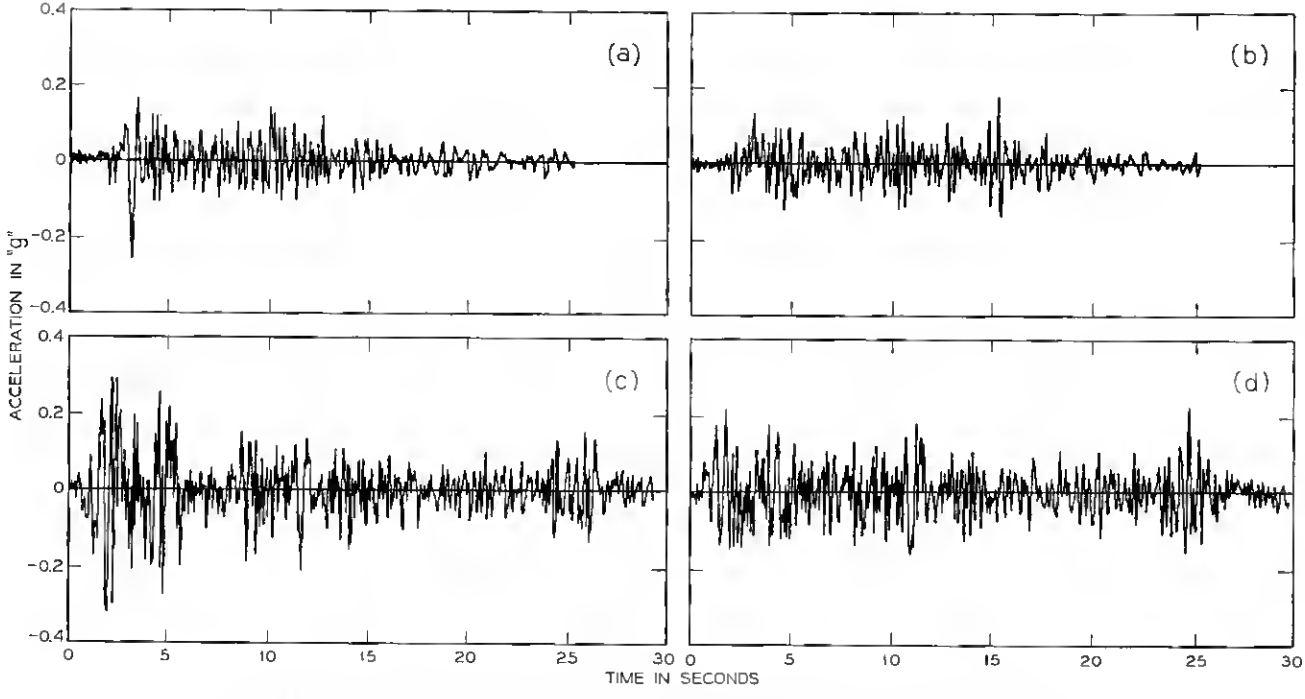

Fig. 1—Strong motion earthquake accelerograms. El Centro, Calif., Dec. 30, 1934, (a) N-S, (b) E-W; El Centro, Calif., May 18, 1940, (c) N-S, (d) E-W; Olympia, Wash., Apr. 13, 1949, (e) S10E, (f) S80W; Taft, Calif., July 21, 1952, (g) S21W, (h) N69W; Golden Gate Park, San Francisco, Calif., March 22, 1957, (i) N10E, (j) S80E; Alameda Park, Mexico City, May 11, 1962, (k) N10°46′W, (l) N79°14′E.

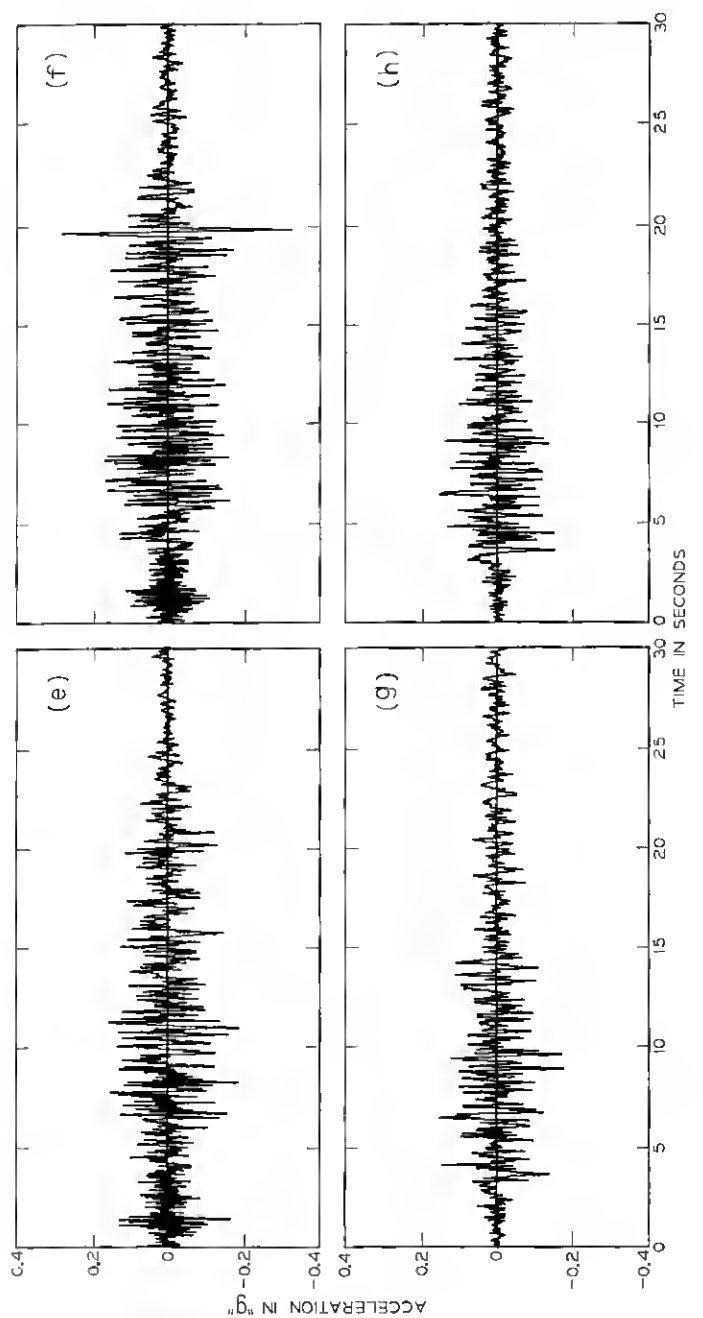
(e)
(f)
(g)
(h)
0.4
0.2
0
-0.2
-0.4
ACCELERATION IN "g"
0
5
10
15
20
25
30
TIME IN SECONDS

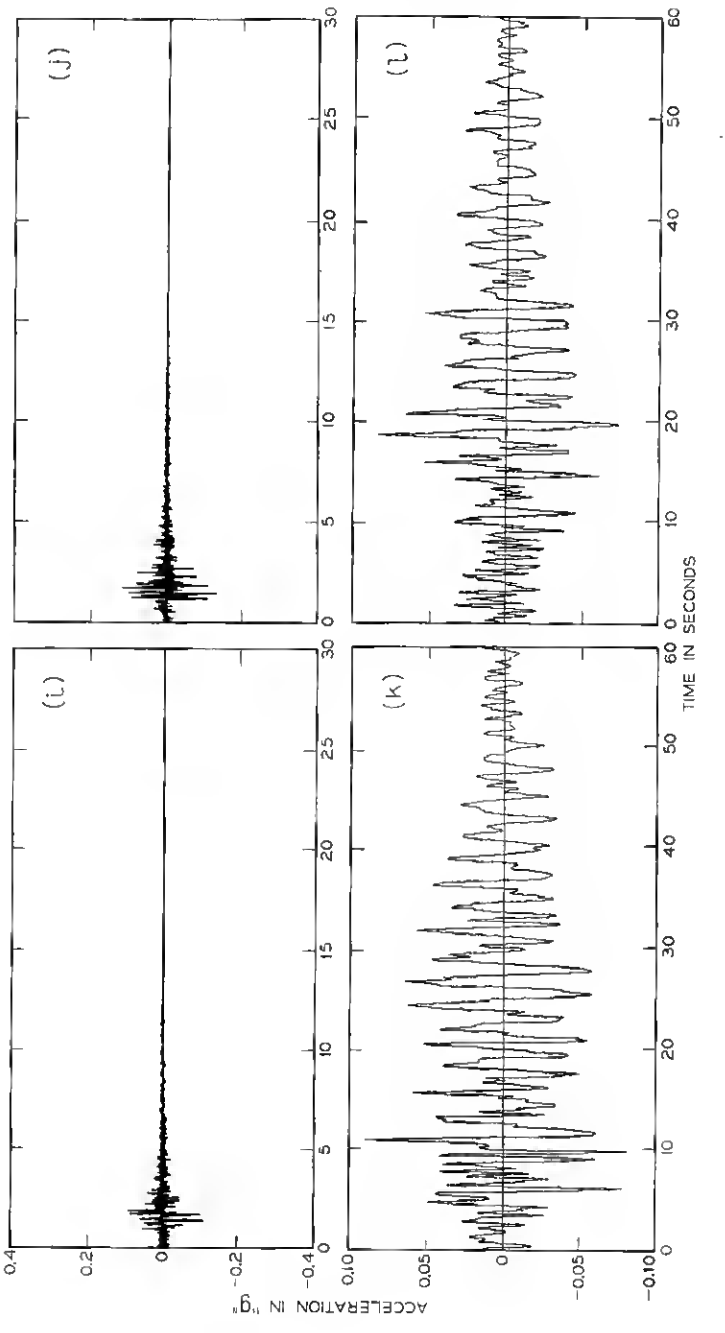
(i)
(j)
(k)
(l)
ACCELERATION IN "g"
TIME IN SECONDS
0.4
0.2
0
-0.2
-0.4
0.10
0.05
0
-0.05
-0.10
0
5
10
15
20
25
30
40
50
60

is debatable, considering the lack of sufficient ground-motion data for statistical studies, the difficulties of establishing valid nonstationary characteristics, and the ultimate objectives in developing a useful stochastic model for earthquake-induced ground accelerations.

The time variations of the rms amplitude of these strong-motion accelerograms are obtained and presented in Fig. 2, from which it is seen that the earthquake rms acceleration in general approaches a stationary value as the duration of the accelerogram is increased. This phenomenon indicates that strong-motion accelerograms are stationary in their rms amplitude at long duration ($T > 20$ seconds, approximately).

The longest and shortest periods existing in a digitized time-history record are $2T$ and $2\Delta t$, respectively. These two extremes constitute an effective period range for the record. Any analysis of the record beyond its effective period range will be of no significance. A Δt of 0.01 second was used in this study.

The stationary rms acceleration can be used to measure the intensity of an earthquake if it is accompanied by the corresponding effective period range. The rms intensities for all earthquakes, assuming $T = 20$ seconds (corresponding to a period range of 0 to 40 seconds), are listed in Table I. This table shows that the N-S component of the El Centro 1940 earthquake (C) has the strongest accelerogram.

It is interesting to compare earthquake rms intensities with the traditionally used Housner intensity,[9] which is defined as

$$SI_\lambda = \int_{0.1}^{2.5} S_v(\lambda, T_o)\, dT_o\,, \tag{12}$$

where S_v is the solution of the following equations:

$$\ddot{u} + \frac{4\pi}{T_o}\lambda\dot{u} + \frac{4\pi^2}{T_o^2}u = -\ddot{x}_g(t) \tag{13}$$

$$S_v(\lambda, T_o) = \max |\dot{u}| \tag{14}$$

for constant coefficients λ and T_o.

Physically, equation 13 represents the equation of motion of a basic single-degree-of-freedom linear system with mass m, viscous damping λ, and stiffness k subjected to earthquake excitation $\ddot{x}_g(t)$ at the support, as shown in Fig. 3. Correspondingly, $T_o = 2\pi\ (m/k)^{1/2}$ is the natural period of the system, and S_v in equation 14 is the maximum relative velocity reached by this system during the earthquake excitation. Therefore, Housner's intensity definition actually represents an

earthquake's potential peak velocity of structures in the period range 0.1 to 2.5 seconds. In Table II the rms (normalized to a factor of 2.7/2.20) and Housner's intensities are compared and good agreements are observed. The basic difference between these two intensity definitions is that the rms intensity is independent of the transfer

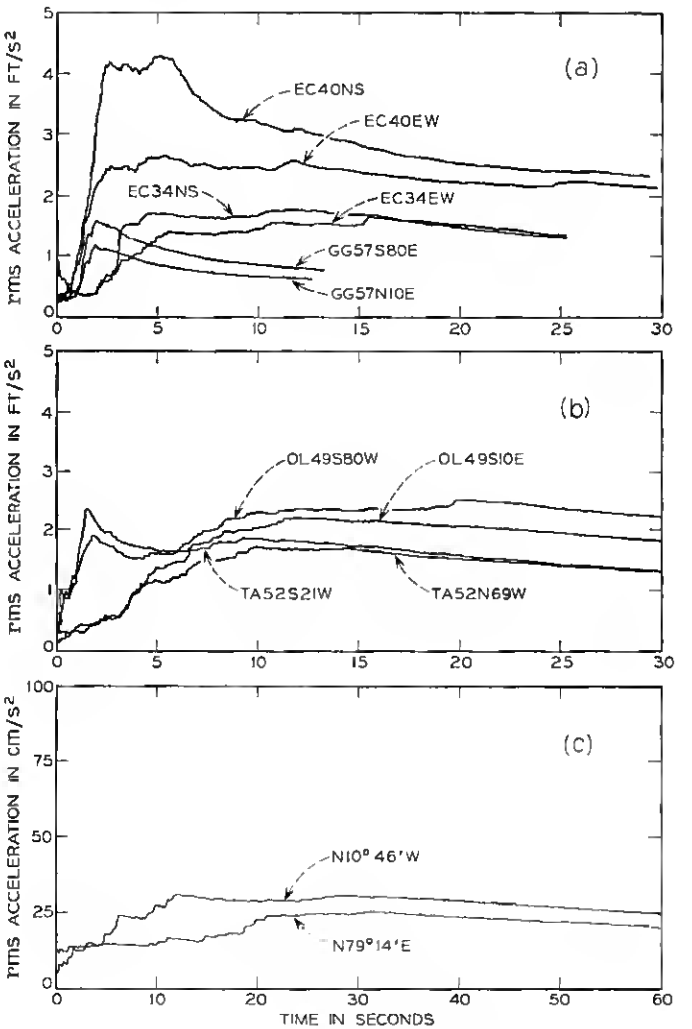

Fig. 2 — Root-mean-square acceleration of strong-motion earthquakes. (a) El Centro and Golden Gate, (b) Olympia and Taft, (c) Alameda Park.

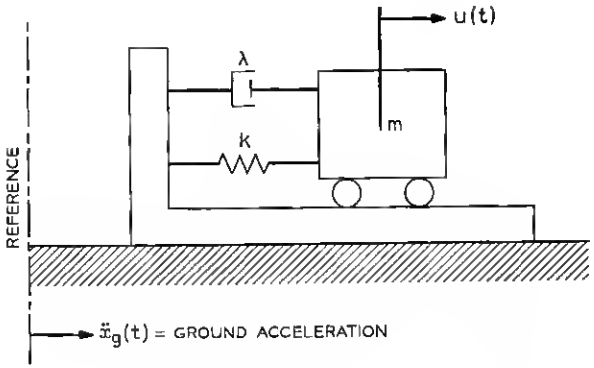

Fig. 3 — Linear mechanical system subjected to ground excitation.

characteristics of the structure while Housner's intensity depends on both the input and the transfer characteristics of the structure. It is much simpler to calculate the rms value for a given input time- history function than to find the SI_λ values, which require numerous mathematical integrations on the computer. However, the rms intensity should be used with care; one should consider the associated effective period range and the predominant period contained in the waveform.

2.2 *Determination of the Predominant Period*

The autocorrelation and power spectral density for all accelerograms considered are found on a digital computer by using a Fortran program

TABLE I — RMS INTENSITIES OF STRONG-MOTION EARTHQUAKES

Cass	Identification	RMS acceleration at T = 20 s (ft/s²)	Average rms (ft/s²)
A	EC34NS	1.4	1.4
B	EC34EW	1.4	
C	EC40NS	2.4	2.20
D	EC40EW	2.0	
E	OL49S10E	1.7	1.85
F	OL49S80W	2.0	
G	TA52S21W	1.4	1.4
H	TA52N69W	1.4	
I	GG57S80E	0.8*	0.7*
J	GG57N10E	0.6*	
K	AL62N10°46′E	0.75	0.725
L	AL62N70°14′E	0.7	

* Taken at T = 10.0 s.

based on equations 10 and 11. Those functions, $R(\tau)$ and $S(\omega)$, for the El Centro 1940 earthquake are shown in Figs. 4 and 5 for the N-S and E-W components, respectively. The smooth curves in the power spectral density diagrams (Figs. 4b and 5b) were obtained by introducing a Hanning or smoothing procedure[10] to the raw estimates given by equation 11. The autocorrelation functions (Figs. 4a and 5a) all have a maximum at $\tau = 0$ and diminish rapidly at large correlation time. The ordinates of the power spectral density functions (Figs. 4b and 5b) generally increase with increasing frequencies to a maximum value at some frequency which may be considered a predominant or characteristic ground frequency, and then decrease rather rapidly toward zero in an asymptotic manner. Also of interest is the fact that this general rise and fall of the power spectral density function is accompanied by local random fluctuations.

The above results indicate that the autocorrelation and power spectral density of strong-motion earthquake accelerograms resemble those of a narrowband process. This implies that earthquake acceleration may be simulated by passing a wideband process through a linear filter which reflects the local geological conditions.

III. STOCHASTIC SIMULATION OF GROUND-MOTION ACCELEROGRAMS

3.1 *Basic Requirements for Ground-Motion Model*

There are many occasions when a ground-motion model is required. Examples are the prediction of ground motion at a certain site where no past records are available, and statistical analyses of structural responses based upon very limited actual ground-motion records. The hypothesized models must, of course, possess the pertinent characteristics of real ground motions and must be supported by existing data. More importantly, these models must properly reflect the damage (or response) potential of future ground motions to a wide range of structures.

TABLE II — COMPARISON OF EARTHQUAKE INTENSITIES

Earthquake case	A & B	C & D	E & F	G & H	I & J	K & L
Normalized rms intensity	1.7	2.7	2.2	1.7	0.84	0.9
Housner intensity	1.9	2.7	1.9	1.6	unavailable	

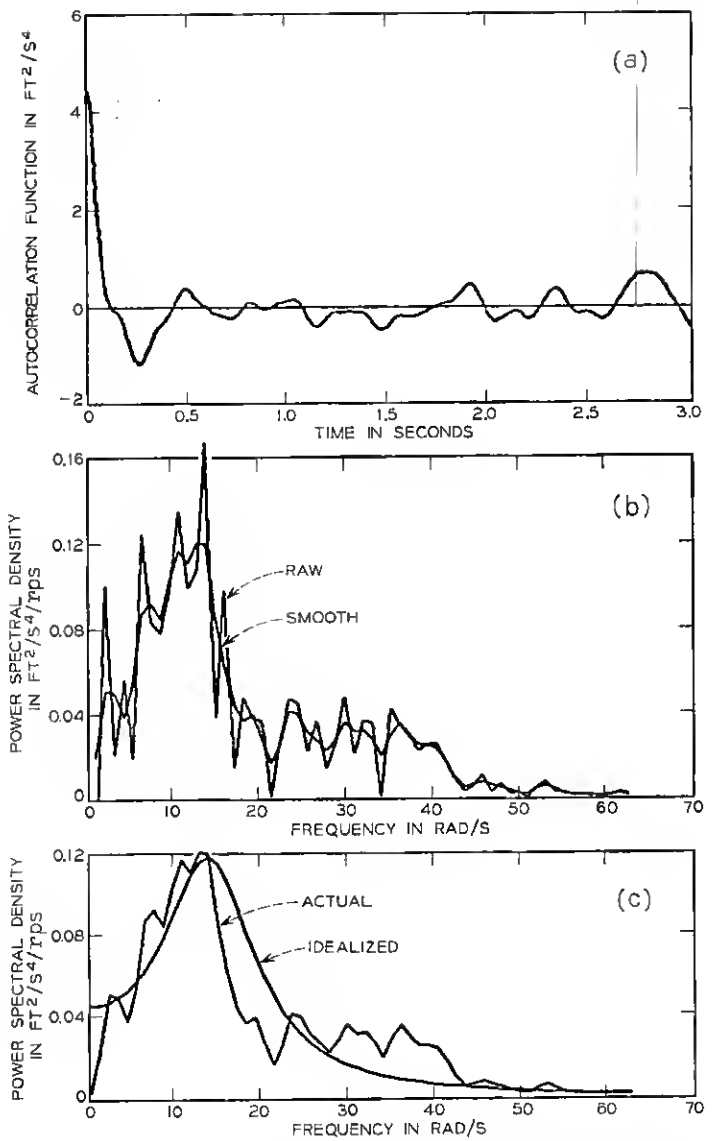

Fig. 4 — N-S component of earthquake at El Centro, Calif., May 18, 1940. (a) Autocorrelation function. (b) Power spectral density function. (c) Comparison of actual and idealized power spectral density functions.

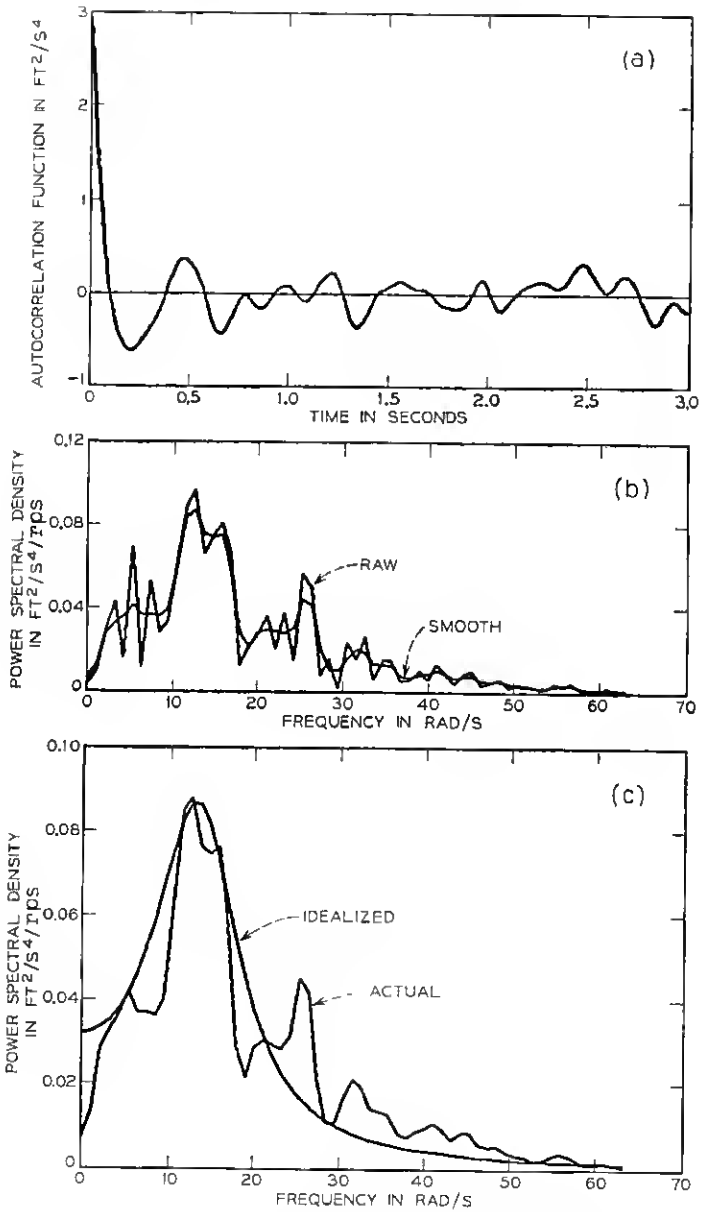

Fig. 5 — E-W component of earthquake, El Centro, Calif., May 18, 1940. (a) Autocorrelation function. (b) Power spectral density function. (c) Comparison of actual and idealized power spectral density functions.

The random phenomenon observed in earthquake ground motions suggests that one can reasonably assume that the resultant seismic wave arriving at the surface of the ground will contain a random assemblage of velocity impulses having gaussian distribution. Furthermore, the analyses of the earthquake accelerograms in the previous sections show that they have characteristics resembling those of a narrowband process. It is therefore postulated that the use of stochastic processes would be appropriate in modeling earthquake ground motions.

Basic criteria for establishing such a stochastic model can be specifically stated as follows:

(*i*) The model must have the basic properties reflected by the past recorded data such as the intensity, duration, general physical appearance, and all important characteristics resulting from local geological conditions.

(*ii*) The response statistics of the stochastic model must be equivalent to those produced by the real ground motion or to those predicated on strong theoretical or empirical bases.

Some simplifying assumptions required in the development of our stochastic model for earthquakes are:

(*i*) The input seismic wave transmited at bedrock by an earthquake is represented by stationary, white noise.

(*ii*) The ground layers of a seismic station during the shock are represented by a single-degree-of-freedom system with linear behavior. (A more sophisticated ground-layer filter may also be used.)

(*iii*) Local random fluctuations appearing in the power spectral density function of the real earthquake accelerogram are neglected when modeling the transfer characteristics of the site.

The representation of ground layers by a single-degree-of-freedom system is sbown in Fig. 6. Sueh a simple system is charaeterized by its transfer function $h(\tau)$ in the time domain or $H(i\omega)$ in the frequency domain, with $h(\tau)$ and $H(i\omega)$ known as the unit impulse response and the complex frequency response of a linear system, respeetively.

If the simple mechanical system shown in Fig. 3 is used as the linear filter, the power spectral density of the total acceleration of the mass, when the acceleration at the support is taken as the input, can be found in terms of the corresponding transfer function.

$$S_o(\omega) = | H(i\omega) |^2 S_i = \frac{S_i[1 + 4\lambda_g^2(\omega/\omega_g)^2]}{[1 - (\omega/\omega_g)^2]^2 + 4\lambda_g^2(\omega/\omega_g)^2} \tag{15}$$

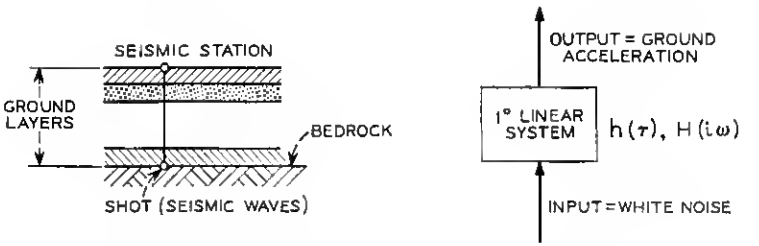

Fig. 6 — Ground layers represented by a linear system.

where S_i is the constant power spectral density of the input acceleration hy assumption (i); λ_g and ω_g are the ground characteristic damping and frequency, respectively.

For known S_i , λ_g , and ω_g , equation 15 gives a smooth curve for $S_o(\omega)$. The location of the peak amplitude of $S_o(\omega)$ is determined hy ω_g . The shape or the rate of the rise and fall of $S_o(\omega)$ is governed hy λ_g , and the relative amplitude of $S_o(\omega)$ depends on S_i . For any power spectral density derived from a real ground-motion record, an idealized, smooth equivalent power spectral density can he found hy using equation 15 and by properly adjusting the three-characteristic constant λ_g , ω_g , and S_i in this equation. The idealized power spectral density function for hoth horizontal components of the El Centro, California 1940 earthquake were found hy the prescrihed procedure. As shown in Figs. 4c and 5c for hoth cases, the idealized power spectral density function covers the same area as the actual power spectral curve in the frequency range 0 through 10 cps. The ω_g , λ_g , and S_i values used for the N-S and E-W components of the El Centro 1940 earthquake are 15.5 rad/s, 0.42, 0.046 ft^2/s^4/rps, and 14.7 rads/s, 0.41, 0.033 ft^2/s^4/rps, respectively.

Once the representative ground-layer filter for a given ground motion is determined, the artificial earthquake can he generated by passing white noise through this filter and measuring the output time history.

3.2 *Generation of a Gaussian Stationary Process*

This procedure starts by sampling a sequence of pairs of statistically independent random numbers $x_1, x_2; x_3, x_4; \cdots; x_{n-1}, x_n$ all of which have a uniform probability distribution over the range $0 < x < 1$. A new sequence of pairs of statistically independent random numbers $y_1, y_2; y_3, y_4; \cdots; y_{n-1}, y_n$ are then generated using the relations

$$y_i = (-2 \log_e x_i)^{\frac{1}{2}} \cos 2\pi x_{i+1} \qquad i = 1, 3, \cdots, n-1 \qquad (16)$$

$$y_{i+1} = (-2 \log_e x_i)^{\frac{1}{2}} \sin 2\pi x_{i+1}$$

which have been shown to have a gaussian distribution with a mean of zero and a variance of unity.[11-13]

A single waveform $y(t)$ can now be established by assigning the values $y_1, y_2 \ldots, y_n$ to n successive ordinates spaced at equal intervals Δt along a time abscissa and by assuming a linear variation of ordinates over each interval. To define a time origin, assume that the initial ordinate y_o, which is taken equal to zero, is located at $t = t_o$ where t_o is a random variable having a uniform probability density function of intensity $1/\Delta t$ over the interval $o < t_o < \Delta t$.

For practical reasons Δt must, of course, be taken as finite; however, its value should be set sufficiently small so that the true power spectral density function is reasonably constant at intensity S_i over the lower range of frequencies which are to be properly represented in the process. A value of 0.025 second or smaller is recommended.

To establish the desired stationary process $a(t)$, each member $y_r(t)$ $(r = 1, 2, \cdots, N)$ of the normalized process $y(t)$ must be filtered in accordance with equation 15. This step can be accomplished by assuming that a simple single-degree-of-freedom system having an undamped circular frequency ω_s and a damping ratio λ_s is subjected separately to the N support accelerations $y_r(t)$ and then by calculating the corresponding absolute or total acceleration functions $a_r(t)$ of the mass. In mathematical form this statement is equivalent to saying that one must solve the differential equations

$$\ddot{Z}_r(t) + 2\omega_s\lambda_s\dot{Z}_r(t) + \omega_s^2 Z_r(t) = -y_r(t) \qquad r = 1, 2, \cdots, N \qquad (17)$$

for the functions $\ddot{Z}_r(t)$ and then evaluate the desired family of acceleration functions $a_r(t)$ using the relation

$$a_r(t) = \ddot{Z}_r(t) + y_r(t) \qquad r = 1, 2, \cdots, N. \qquad (18)$$

Equation 17 can be solved numerically on a digital computer using the standard linear acceleration method. Based on the assumption that the input earthquake duration is divided into the very short equal time intervals Δt, and the response acceleration varies linearly over each interval, this method gives the following simple relations between the response displacement Z_r and its derivatives at step n and $n+1$:

$$(\dot{Z}_r)_{n+1} = (\dot{Z}_r)_n + \frac{(\ddot{Z}_r)_n}{2}\,\Delta t + \frac{(\ddot{Z}_r)_{n+1}}{2}\,\Delta t$$

$$(Z_r)_{n+1} = (Z_r)_n + (\dot{Z}_r)_n\,\Delta t + \frac{(\ddot{Z}_r)_n}{3}\,\Delta t^2 + \frac{(\ddot{Z}_r)_{n+1}}{6}\,\Delta t^2. \qquad (19)$$

IV. ILLUSTRATIONS OF GENERATION OF ARTIFICIAL ACCELERATION

4.1 *By Known Power Spectral Density*

As the first example, artificial earthquakes are generated using the prescribed approach, to simulate the average of U. S. strong-motion earthquakes observed at seismic stations having a firm soil foundation. Values of 15.6 rad/s for ω_g and 0.6 for λ_g, representative of such soil conditions, were used. A total of 50 artificial accelerograms ($N = 50$) were generated for process $a(t)$ with a duration of 30 seconds which corresponds to $\Delta t = 0.025$ second and $n = 1200$. The intensity S_i of the unfiltered "white noise" was set at 0.00614 ft²/s³ so that the mean velocity response spectrum curves for the filtered process $a(t)$ would give a "best fit" with the standard response spectrum curves published by G. Housner.[9] This intensity is slightly less than the value of 0.0063 ft²/s³ used by J. Penzien[14] in a previous investigation to correlate the mean velocity response spectrum curves for "white noise" with Housner's standard curves.

A typical sample member of artificial accelerograms generated is shown in Fig. 7. It is interesting that this accelerogram appears to be very similar to the real accelerograms in Fig. 1 except for the general

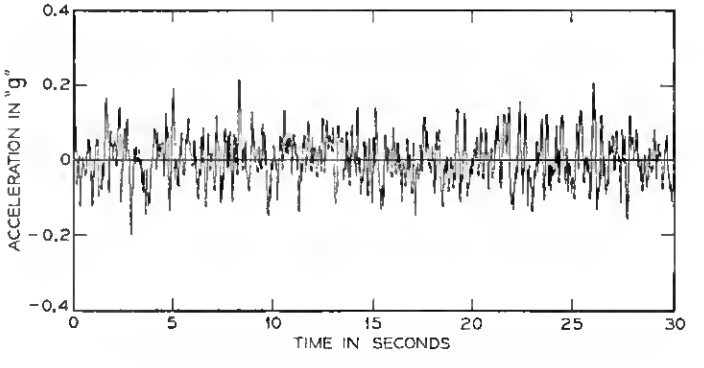

Fig. 7 — Sample member of artificial accelerogram.

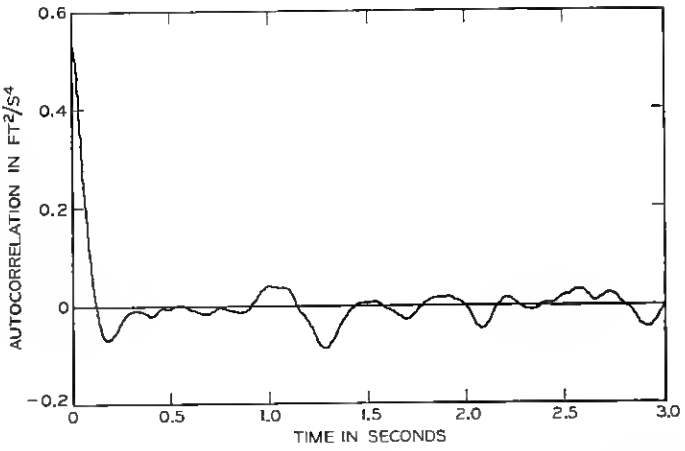

Fig. 8 — Autocorrelation function of the sample member of artificial accelerogram.

stationary apparance of the artificial accelerograms versus the nonstationary appearance of the real accelerograms.

The autocorrelation and corresponding power spectral density function for this sample artificial earthquake are shown in Figs. 8 and 9, respectively. It is of particular significance that, while these autocorrelations and power spectral densities are similar to those for the real earthquake (Figs. 4 and 5), local random fluctuations also appear in

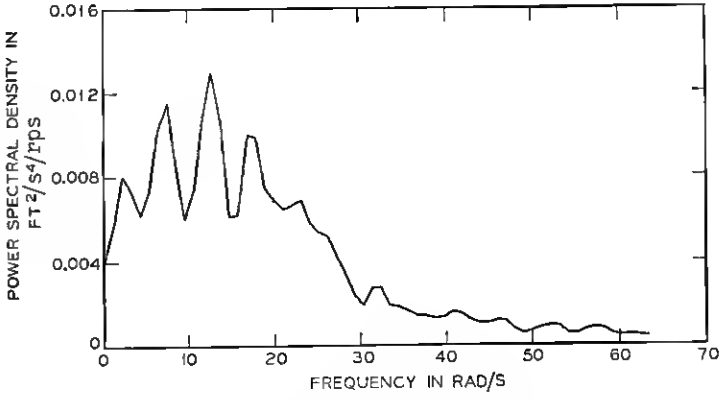

Fig. 9 — Power spectral density function of the sample member of artificial accelerogram.

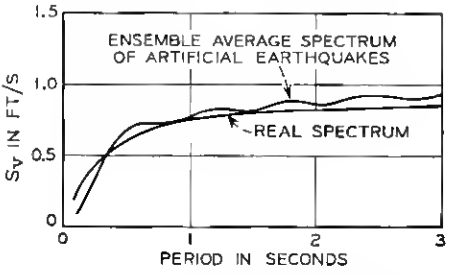

Fig. 10 — Comparison of velocity spectra of earthquakes, $\lambda = 0.02$.

the individual power spectral density function. It is expected that these local fluctuations and the variations from one individual power spectral density function to another will be eliminated by the averaging procedure. It has been shown that the average power spectral density function of artificial earthquakes is quite close to the prescribed function.[15]

The average response spectra ($\lambda = 2\%$) of 50 artificial earthquakes are compared with the real spectra given by Housner[9] in Fig. 10. Good agreements are observed over the significant period range. The confidence limits for these average spectra are given in Fig. 11 by extending 3σ (standard deviation) of S_v above and below the mean. Since the distribution of the response spectra is no longer gaussian, these limits correspond to an approximate 89 percent confidence band according to Chebyshev inequality.[16, 17]

The above results (Figs. 7 through 11) show that the basic require-

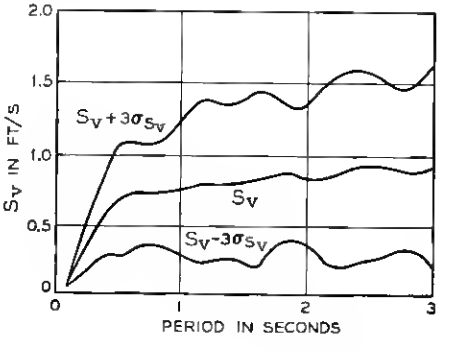

Fig. 11 — Variations and confidence limits for average velocity spectra of artificial earthquakes, $\lambda = 0.02$.

ments for ground-motion simulation have been satisfied. It takes approximately 10 seconds to generate one sample function on a CDC 6600 digital computer. These facts indicate that a good, reasonably economical ground-motion simulation has been achieved.

4.2 *By Known Response Spectrum*

In the second example, we have a situation somewhat different from the first. Engineers are asked to generate representative ground-motion accelerations from an estimated pseudovelocity spectra as given in Fig. 12. There is no past recorded ground-motion data available. The generated artificial earthquakes will be used to evaluate the probable damage of structures resulting from possible seismic events tak-

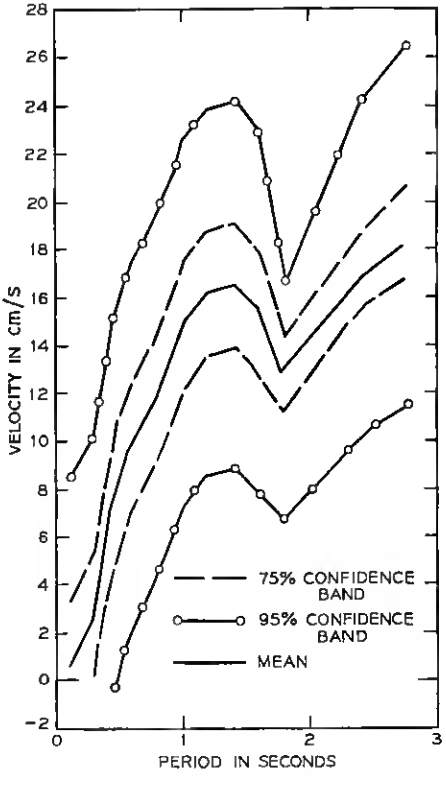

Fig. 12 — Pseudovelocity response spectra, $\lambda = 0.02$.

ing place in the vicinity of a proposed site. The estimated response spectra were obtained from a careful examination of earthquake activities in a certain seismic area and from an analogous prediction using records taken at stations having geological conditions similar or comparable to those of the given site. If the event refers to an underground explosion, the estimated response spectra might be predicted from past events under the same physical conditions (yield level and depth of the explosion, epicenter distance, and so on) and similar geological environments.

The given pseudoresponse spectrum curves (Fig. 12) show peaks at period $T_o \cong 1.25$ seconds if the long-period portion ($T_o > 2.5$ seconds) or the low-frequency portion ($\omega_o < 2.5$ rad/s) is neglected. The corresponding frequency value where the peak spectrum amplitudes occur is approximately 5 rad/s. This value can be used as an approximate predominant ground frequency ω_o. The proposed site has a firm soil foundation, therefore a value of 0.6 for the characteristic ground damping λ_o is used.

Using these two characteristic values and letting S_i be unity in equation 15, the same procedure as used in the first example can be followed again. Five typical artificial accelerograms of 30-second duration are generated and shown in Fig. 13. The individual response spectra and the mean response spectra are obtained (Fig. 14). The general shape of the pseudoresponse spectra using $S_i = 1.0$ is similar to the estimated spectra. By matching the area covered by the estimated and pseudospectra curves, the amplitudes of the pseudospectra are normalized to have the same order of magnitude as the estimated spectra. The accelerations shown in Fig. 13 which have been modified by these same normalization procedures, represent the final form of the desired artificial accelerograms.

The comparisons of individual and mean pseudoresponse spectra with the given response spectra (Fig. 14) are satisfactory except for the high-period range ($T_o > 2.5$ seconds). If only those general building structures are considered which have a natural period range of 0.3 to 2.5 seconds, the large discrepancy of response spectra in the high-period range is not significant. The mean pseudoresponse spectrum (Fig. 14f) gives better results, as is expected. Overall results of the simulation may be improved with more accurate determination of values for ω_o, λ_o, and the larger sample size N of the simulating process. Methods for such improvements are presented in a separate paper.[18]

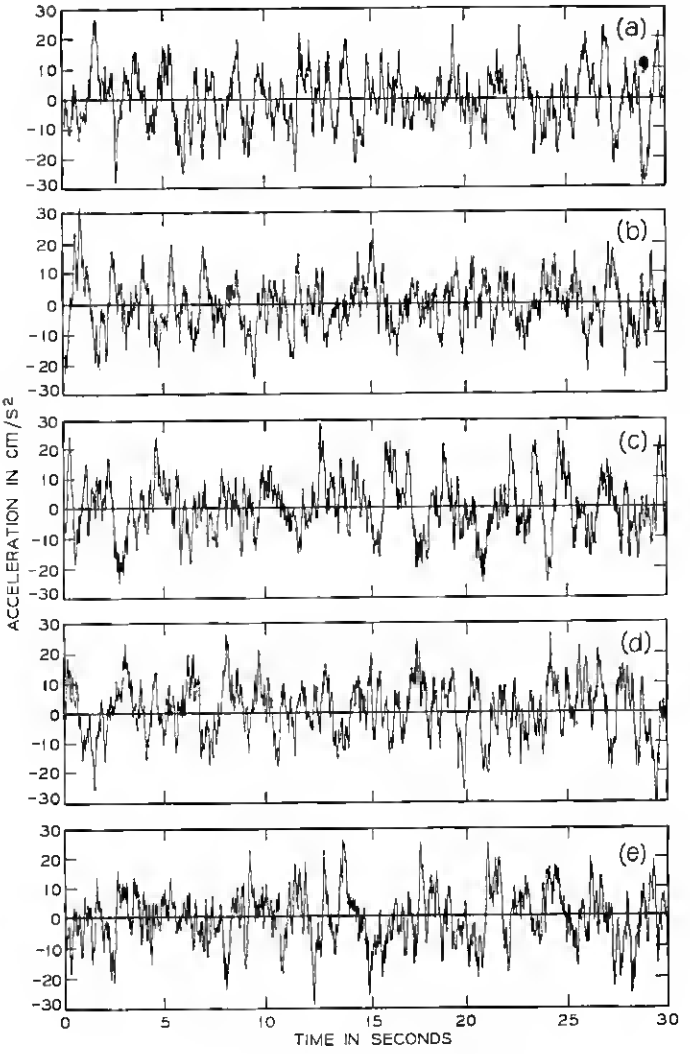

Fig. 13 — Pseudoearthquake accelerograms.

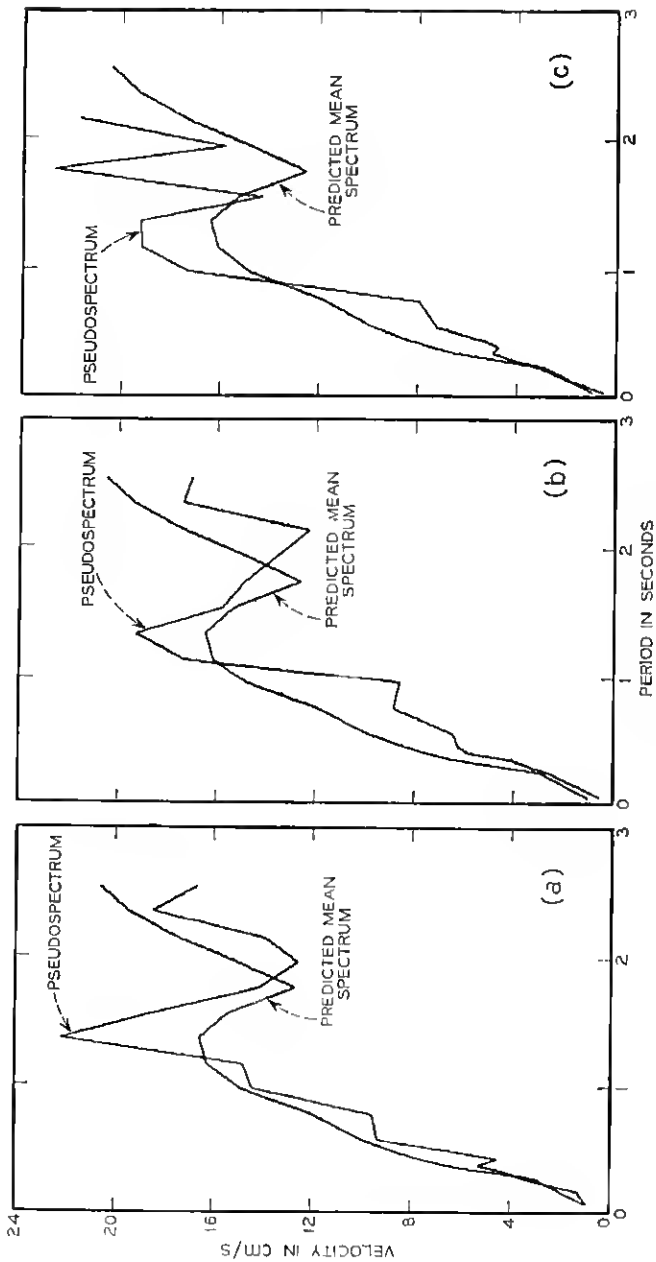

Fig. 14 — Comparisons of velocity response spectra, $\lambda = 0.02$.

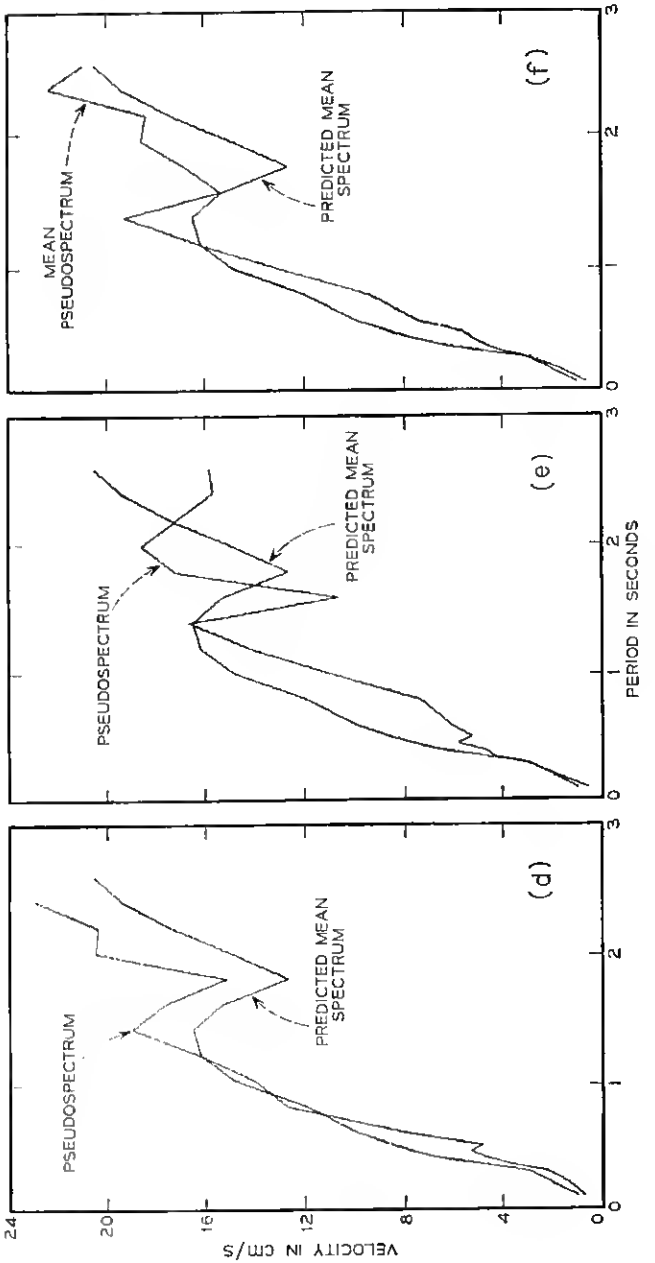
(d)
(e)
(f)
PSEUDOSPECTRUM
PREDICTED MEAN SPECTRUM
MEAN PSEUDOSPECTRUM
VELOCITY IN CM/S
PERIOD IN SECONDS
0
4
8
12
16
20
24
1
2
3

V. CONCLUSIONS

From the results presented in this investigation, the following conclusions may be deduced:

(*i*) In general, strong-motion earthquake accelerograms of sufficiently long duration ($T > 20$ seconds, approximately) are stationary in the rms sense.

(*ii*) The rms acceleration of an earthquake, along with the effective period range and the predominant period of the associated accelerogram, can be used to determine the intensity of tbe earthquake.

(*iii*) The autocorrelation and the power spectral density of a strong-motion earthquake resemble those of a narrowband process.

(*iv*) The power spectral density analysis of existing earthquake records suggests that the transfer characteristics of the given site can be represented by a simple, linear system.

(*v*) A filtered, gaussian, stationary process generated on a digital computer proves to be successful in modeling ground motions induced by earthquakes or by nuclear underground explosions.

VI. ACKNOWLEDGMENTS

The author wishes to express his appreciation for the valuable suggestions given by Professor J. Penzien of The University of California at Berkeley, and for the careful review of the manuscript given by M. Oien, L. W. Fagel, and S. E. Wisnewski of Bell Telephone Laboratories.

REFERENCES

1. Alford, J. L. and Housner, G. W., "Spectrum Analyses of Strong-Motion Earthquakes," Research Rep., Earthquake Eng. Res. Laboratory, California Inst. of Tech., Pasadena, Calif., August 1951.
2. Bycroft, G. N., "White Noise Representation of Earthquakes," Proc. Amer. Soc. Civil Engineers, *86*, No. EM2 (April 1960), pp. 1–16.
3. Housner, G. W. and Jennings, P. C., Jr., "Generation of Artificial Earthquakes," Proc. Amer. Soc. Civil Engineers, *90*, No. EM1 (February 1964), pp. 113–150.
4. Bogdanoff, J. L., Goldberg, J. E., and Bernard, M. C., "Response of a Simple Structure to a Random Earthquake-Type Disturbance," Bull. Seismological Soc. Amer., *54*, No. 1 (February 1964), pp. 263–276.
5. Caughey, T. K. and Stumpf, H. J., "Transient Response of a Dynamic System Under Random Excitation," J. Appl. Mechanics, Trans. Amer. Soc. Mechanical Eng., *28*, No. E-4 (December 1961), pp. 563–566.
6. Amin, M. and Ang, A. H. S., "A Nonstationary Stochastic Model for Strong Motion Earthquakes," Technical Rep. *306*, Civil Engineering Studies, University of Illinois, April 1966.

7. Ward, H. S., "Analog Simulations of Earthquake Motions," Proc. Amer. Soc. Civil Engineers, *91*, No. EM5 (October 1965), pp. 173–190.
8. Shinozuka, M. and Sato, Y., "Simulation of Nonstationary Random Process," Proc. Amer. Soc. Civil Engineers, *93*, No. EM1 (February 1967), pp. 11–40.
9. Housner, G. W., "Behavior of Structures During Earthquakes," Proc. Amer. Soc. Civil Engineers, *85*, No. EM4 (October 1969), pp. 109–129.
10. Blackman, R. B. and Tukey, J. W., *The Measurement of Power Spectra*, New York: Dover Publications, Inc., 1958, pp. 14–37.
11. Box, G. E. P. and Miller, M. E., "A Note on the Generation of Random Normal Deviates," Ann. Math. Stat., *29*, No. 2 (June 1958), pp. 610–611.
12. Franklin, J. N., "Deterministic Simulation of Random Processes," Math. of Computation, *17*, No. 81 (January 1963), pp. 28–59.
13. Franklin, J. N., "Numerical Simulation of Stationary and Nonstationary Gaussian Random Processes," SIAM Review, *7*, No. 1 (January 1965), pp. 68–80.
14. Penzien, J., "Applications of Random Vibration Theory in Earthquake Engineering," Bull. Int. Inst. Seismology and Earthquake Eng., *2* (1965), pp. 47–69.
15. Liu, S. C., "Nondeterministic Analysis of Nonlinear Structures Subjected to Earthquake Excitations," Ph.D. dissertation, University of California, Berkeley, 1967.
16. Bendat, J. S., "Mathematical Analysis of Average Response-Values for Nonstationary Data." IEEE Trans. BioMedical Eng., *BME-11*, No. 3 (July 1964), pp. 72–81.
17. Bendat, J. S. and Thrall, G. P., "A Summary of Methods for Analyzing Nonstationary Data," NASA Technical Report 32-744, Jet Propulsion Laboratory, California Institute of Technology, Pasadena, California, September 1, 1965. p. 4.
18. Liu, S. C. and Jhaveri, D. P., unpublished work.